J. Fluid Mech. (1987), *vol.* 183, *pp.* 185–198
Printed in Great Britain

Experiments on the trajectory and circulation of the starting vortex

By DAVID AUERBACH

Max Planck-Institut für Strömungsforschung, Bunsenstr. 10, D-3400 Göttingen, Federal Republic of Germany

(Received 31 May 1986 and in revised form 1 December 1986)

Various reasons have been given as to why the trajectories and circulations of vortices generated at sharp edges do not follow classical similarity-theory predictions for at least an initial short time. Amongst these are the effect of the particular flow geometry (e.g. duct with wedge, nozzle) distant from the salient edge (for rectilinear vortices); axisymmetry (for ring vortices); end effects (for rectilinear vortices); viscous diffusion; finite thickness of the detaching shear layer, as well as secondary vorticity caused by the interaction of the primary vortex with the edge at which it was generated. A further process that may be active is that of viscous entrainment. Experiments, in which essentially straight-line vortices were generated, indicate that of the seven possibilities mentioned, the first five do not play a significant part. All models consist of a basic flow onto which the modelled vortex is superposed. Thus either the basic flow or the vortex model are at fault. The basic flow onto which the vortex is superposed may well not be a pure edge flow, but one that is already taking on the character of an entraining jet flow. On the other hand, the vortex model fails to incorporate secondary vorticity which, particularly when rolled up, might be expected to be dynamically important.

1. Introduction

During the past few years certain seemingly contradictory results have been obtained, both for predictions and measurements of the motion and circulation of vortices generated at a sharp edge. Thus, for example, a student wishing to know the initial lift of an impulsively starting cusped aerofoil (edge angle $\gamma = 0°$), will find values in the literature ranging from zero to infinity (see Graham 1983), depending on how the starting vortex is chosen to move! The two lines of thought leading to this extreme discrepancy both model such a starting vortex as an infinitely thin vortex sheet in an otherwise inviscid flow (the question as to whether this problem is well-posed is still unsolved). The line of thought (e.g. Graham 1983) leading to the ∞-value assumes a self-similar potential flow† near the edge for an 'embryonal' time t_e of the order L/V (L, some typical length; V, some typical velocity), after which the geometry distant from the edge will dominate the flow. On the other hand the line of thought leading to the 0-value (e.g. Chow & Huang 1982) considers the distant geometry to be important *ab initio* to the flow at the edge – the flow can never be considered self-similar. The most obvious kinematic consequence is that the initial path of the vortex centre must be straight for the former model, whereas generally curved for the latter.

† One that may be made steady by a transformation using powers of the time only.

Now although earlier experiments (Kaden 1931; Wedemeyer 1961) on the trajectory of real starting vortices indicated that they may behave in a self-similar fashion, more recent experiments (Didden 1979, 1982; Pullin & Perry 1980; Blondeaux & De Bernadinis 1983) indicate the contrary. The above explanation for this non-self-similar behaviour, used for example by Blondeaux & De Bernadinis (1983), has the following major problem: that an inviscid starting edge flow embedded in some geometry which may be considered distant from the salient edge has been more or less tacitly tackled using matched asymptotic expansions. Here the flow is effectively divided into two regions, an inner region near the edge, where the flow is dominated by the growing vortex, and an outer region, in which the flow is determined by the steady potential describing the inviscid flow through or about that particular geometry. Matching is done by taking the usual limits and equating in the known fashion, from which the constants in the resulting formulae are obtained, whereby the question as to the extent of the overlap region is not easy to solve. We shall see that the line of thought mentioned at the outset predicting a non-self-similar vortex roll-up *ab initio* effectively recognizes no such inner region insofar as the source of this non-self-similarity is thought to lie in the outer flow.

There are other perhaps more persuasive reasons as to how a characteristic length could enter the problem from the beginning of the motion. An axisymmetric geometry, such as that used to generate ring vortices, will introduce a length, the radius of curvature, into the problem from the outset. For real rectilinear vortices, the flow induced by the existence of the ends may affect the flow elsewhere. Viscous diffusion too might introduce a length which will grow as $(\nu t)^{\frac{1}{2}}$. Another process, mentioned by Pullin & Perry (1980), is that of secondary-vortex generation at the edge (see also Walker 1978). Such generation would obviously affect the primary vortex so long as the two were of comparable size. Also, secondary vorticity, even if it does not roll-up, causes both the already finite thickness of the shear layer to increase, and the total effective circulation generated at the edge to reduce. A final process that we shall discuss is that of viscous entrainment.

2. Analysis

If the steady potential flow for the geometry in question is $W = F(z')$, where $z' = x' + \mathrm{i}y'$ is based on the coordinates of the edge-centred frame of reference shown in figure 1 (*a*), using the local lengthscale $s = (\Gamma(t)\, t)^{\frac{1}{2}}$, the potential W_1 for the inner flow is

$$W_1 = \Gamma(t)\, W\left(\frac{z'}{(\Gamma(t)\, t)^{\frac{1}{2}}}\right).$$

For geometries where Schwartz–Christoffel-type transformations can be used, if the origin is taken to be the salient edge, the outer potential $W_0 = W$ consists of a series with generally complex coefficients. We may then write the leading term as

$$F_0 = -\mathrm{i}qVL\left(\frac{z'}{L}\right)^n, \tag{1}$$

with q real; L the typical length, and $1/n = 2 - \gamma^\circ/180$. The flow in (1) is called asymmetric since it transforms to a constant translational flow with velocity V in the (ξ, η)-plane (i.e. a flow not symmetric about the ξ-axis) under the transformation $z = \zeta^{1/n}$ with $\zeta = \xi + \mathrm{i}\eta$. The asymmetric quality of this potential is indicated by the arrows in figure 1 (*a*). Pullin (1979) considered the case of a vortex growing at a nozzle

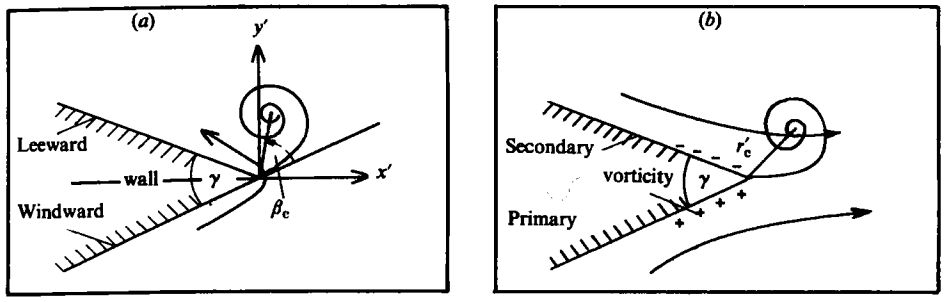

FIGURE 1. Vortex growth at an edge. In (*a*) the asymmetric *V*-, and in (*b*) the symmetric *U*-component predominates.

of width or diameter L, the flow being set into motion by a piston moving with velocity $V = U_p$. Now the above constant q is determined by the overall geometry of the flow. He calculated q to be $1/(2\pi)^{\frac{1}{2}}$ for an axisymmetric nozzle, compared to the classic $1/\pi^{\frac{1}{2}}$ for the corresponding two-dimensional nozzle (both with $\gamma = 0°$).

If we take only the leading term, (1), into consideration, $W_0 = F_0$. Using the matching idea, the outer flow behaves as (1) as $z' \to 0$. From the form of the potential W_0 above, we can write the inner potential W_1 to leading order as

$$W_1 = -ip\Gamma(t)\frac{z'^n}{\{\Gamma(t)\,t\}^{n/2}}$$

as $z' \to \infty$. Matching inner and outer flows yields

$$\Gamma = \left(\frac{q}{p}\frac{Vt}{L}\right)^{2/(2-n)}\frac{L^2}{t}$$

and

$$s = \left(\frac{q}{p}\frac{Vt}{L}\right)^{1/(2-n)} L.$$

Now p is a constant determined by the local flow situation. Pullin (1978) considered this to be that constant determined by the vortex model alone (e.g. point vortex, spiral). He calculated p for a vortex model including the effect of the spiral form for the rolling up sheet (the simple point-vortex representation was developed by Brown & Michael 1955). In order to do this he wrote s in the form

$$s = \left(q\frac{Vt}{L}\right)^{1/(2-n)} L, \tag{2}$$

s now being independent of the vortex model owing to the removal of p. He described p above in terms of two vortex-model-dependent constants ρ and J, and sought a solution z'_c as

$$z'_c = Cs\Omega \tag{3}$$

for the position of the vortex centre. Here $\Omega = \rho\, e^{i(\beta_c - \gamma/2)}$ is the complex shape function; ρ is the non-dimensional model-dependent radius and β_c is the angle that the line r'_c (see figure 1) of length $|z_c|$ makes with the projection of the windward wall. The factor $C = \{(2-n)(1-n)\}^{1/(2-n)}$ keeps Ω finite for all edge angles. According to (3) the vortex centre will move as

$$\{x'_c; y'_c\} = \{\mathrm{Re}\,(Cs\Omega); \mathrm{Im}\,(Cs\Omega)\}, \tag{4}$$

at a constant angle β_c to the edge, the components being the real and imaginary arguments of z_c'. For a point vortex

$$\beta_c = \frac{1}{n}\arccos\left(\frac{1}{2n^{\frac{1}{2}}}\right) - 90\left(2-\frac{1}{n}\right). \tag{5}$$

Such a vortex generated at an edge ($\gamma = 0°$), for example, would move along a straight line at right angles to the edge ($\beta_c = 90°$), its centre having coordinates

$$\{x'; y'\} = \{0(Vt)^{\frac{1}{3}}; 0.669(Vt)^{\frac{1}{3}}\}. \tag{6}$$

Pullin's (1978) inclusion of the spiral changes (6) to

$$\{x'; y'\} = \{0.155(Vt)^{\frac{1}{3}}; 0.701(Vt)^{\frac{1}{3}}\},$$

β_c being 102.5° instead of 90° for $\gamma = 0°$. The circulation Γ becomes

$$\Gamma = C^n J\frac{s^2}{t}, \tag{7}$$

where J is the vortex-model-dependent non-dimensional circulation. We note that by (2), since the constant q_0 taking the geometry into account is found in s only, by (3) and (7) s cancels out of the non-dimensional trajectory $r_c'/(\Gamma t)^{\frac{1}{3}}$. Pullin's (1978) formulation thus predicts identical scaled trajectories for planar and axisymmetric geometries. This is perhaps somewhat surprising since, at least for the case of vortices distant from the generating edges, one would expect the velocity of a ring to be greater than that of an equivalent pair (ratio $O[\log 8R/c]$, where R/c is the ratio of ring-to-core radii). The tacit implication is thus that the circulation decreases with decreasing radius in such a way that $r_c'/(\Gamma t)^{\frac{1}{3}}$ remains constant – a claim that begs experimental verification.

Recognizing the fact that there may be flows where a quantity such as the angle of the flow distant from the edge might enter into the local edge problem as posed in the above fashion, Graham (1977, 1983) included this aspect of the distant flow via the angle of incidence of an aerofoil: the distant flow varies as $U = U_\infty \cos\alpha$ and $V = U_\infty \sin\alpha$, where α is the angle of attack and U_∞ is the (constant) distant flow. He suggested that one could superpose the symmetric potential

$$F_0' = qUL\left(\frac{z'}{L}\right)^{2n}$$

(stagnation flow symmetric about the ξ-axis under the abovementioned transformation with characteristic velocity U) as indicated by the arrow in figure 1(*b*), onto the asymmetric potential (1), yielding

$$\tilde{F}_0 = F_0 + F_0'. \tag{8}$$

He suggested that the second term in (9) might dominate for a wing that begins heaving in a steady flow. If it does, then for sharper edges, F_0' will be the relevant potential, and the point-vortex centre's coordinates become

$$\{x_c'; y_c'\} = \left\{\left(\frac{4n(1-n)\,Ut}{1+n}\right)^{1/2(1-n))}; 0\right\} \tag{9}$$

in place of those given in (6) – the vortex advects passively in the U-field. Graham emphasized, however, that the first term would be dominant for starting flows. Thus, if (1) adequately describes the outer flow, we should expect (4), (5) and (7) to describe vortex motion for a time of at most t_e of the order of L/V. For after this time terms

(with both real and imaginary components) of higher order will dominate the vortex motion, thereby causing the flow to lose its self-similarity.

Now t_e is the upper bound for the above considerations to hold. The lower bound can be obtained by comparing typical viscous- with inviscid-length growth rates. Comparing $(\nu t)^{\frac{1}{2}}$ with s as in (2), one sees that viscous effects might be expected for an initial time t_v. This time, however, turns out to be small. For example, an impulsively started flow with $\gamma = 0°$; $L = 30$ mm; $V = 30$ mm/s and $p/q = 1$ in water yields $t_v = 1.4$ ns. Dropping the assumption of the impulsively started flow implicit in (2) increases this time considerably. For the acceleration times used in this experiment, however, the time during which viscous flow conditions should hold sway according to the above consideration remains insignificantly small.

How do experiments corroborate these predictions? Didden (1979, 1982) measured both trajectories, as well as the circulation of ring vortices generated at a nozzle with $\gamma = 0°$. He found the trajectories to be curved until the ring was completely formed. Further, the initial circulation was substantially smaller than that predicted by (7). The power to which the time had to be raised was substantially larger than that predicted by (7). He accredited these discrepancies to the difference between plane and axisymmetric geometries. Yet, as mentioned above, according to Pullin (1979) the symmetry should change q only. Blondeaux & De Bernadinis (1983) determined the motion of the centre of a single vortex generated at the edge of the asymmetric nozzle ($\gamma_r = 0°$; $\gamma_f = 180°$; $H = 25$ mm; $W = 10$ mm) shown in figure 2 – the nozzle end of the apparatus used in this experiment. Their apparatus differed from Didden's (1979) not only in that it was rectangular, while his was axisymmetric, but also in that there was only one edge for vortex generation rather than two – which would have been the rectilinear pendent to the vortex ring. Nonetheless they too found the vortex trajectories to be always curved: Didden's time power for the x' component was $\frac{2}{3}$, theirs 1. The time power for the y' component was $\frac{2}{3}$ for both – that predicted by (6). Blondeaux & De Bernadinis (1983), however, argued that, since the geometry was asymmetric, a weak symmetric U-component (see figure 1*b*) would be introduced into the flow which would significantly change the trajectory from the beginning. They thus used y' as in (4), but x' as in (9) – the law arising from the symmetric flow potential. Pullin & Perry (1980), using a wedge of variable edge angle γ placed in a channel of rectangular cross-section, also found that the trajectories of rectilinear vortices deviated from similarity-theory predictions. They felt the main reason for discrepancies to be the production of secondary vorticity (at the leeward wall, see figure 1) of the opposite sign to that of the primary vortex. Didden (1979) in fact measured this vorticity for the case of ring vortices. A further problem that exists for the case of straight-line vortices is that they are necessarily generated in three dimensions. To what extent we may consider the flow in the mid-plane to be two-dimensional has not yet been clarified.

A final problem is that of entrainment, mentioned at the outset. For once the vortex has disappeared from the edge, an entraining jet has developed. For a laminar jet, one may consider this entrainment process to be of an essentially viscous nature – the shear layers emerging from the edge first draw distant fluid from the sides towards it, then drag this fluid along by virtue of its non-zero viscosity. This entraining effect has been the object of many studies. For example, Taylor (1958) and Kraemer (1971) simulated such a flow using a potential approach. For the far field at the sides of the jet, Kraemer successfully modelled the entraining effect along the edge of the jet with a distribution of sinks. Vortex roll-up is a very different problem. Nonetheless, when a vortex begins to be generated a shear layer emerges and begins rolling up. One

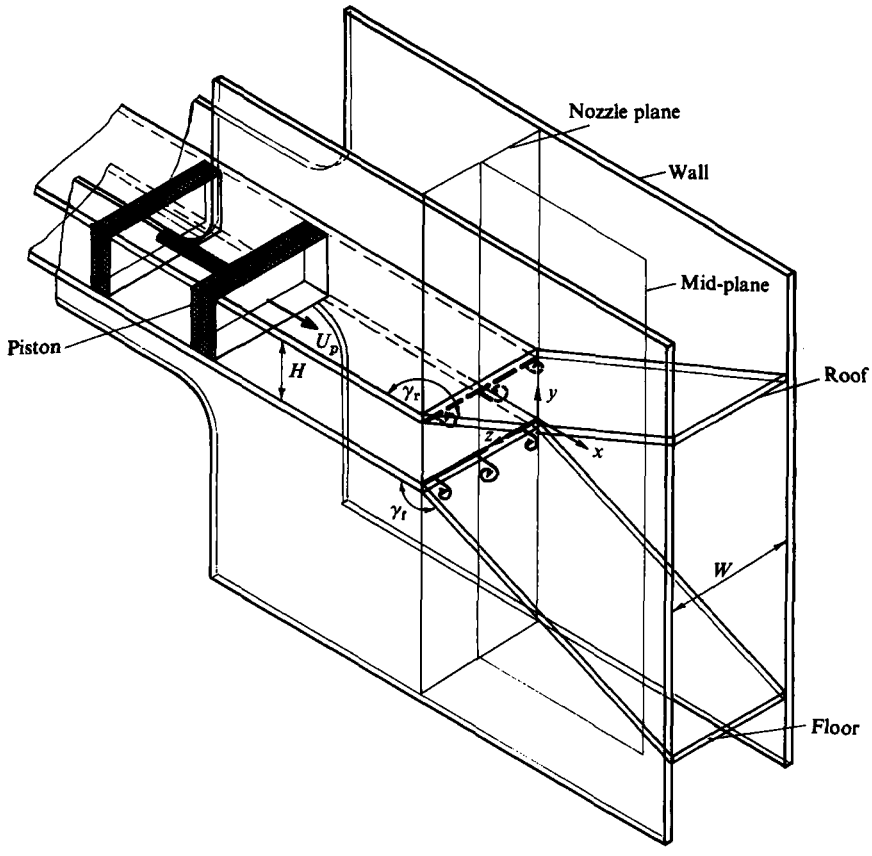

FIGURE 2. Nozzle of the apparatus used, with $H = 30$ mm and $W = 60$ mm.

might, however, expect fluid to be entrained both via a 'Biot–Savart'-type effect due to the vortical nature of the layer, as well as to the abovementioned viscous sink effect. Although the speed with which a typical viscous length would grow is as $(\nu t)^{\frac{1}{2}}$, the sink effect for the above mentioned distant flow will set in directly with the emergence of the shear layer. To what extent this sink effect due to the shear layer should be accounted for, in the formulation of (1), for example, is an open question. Does the shear layer begin entraining in this sense from the beginning, or is there a time in which one may consider this process to be inactive?

Although the list may well not be exhaustive, we have raised seven possible processes that might be important for the non-similar behaviour of the starting vortex:

the effect of the distant geometry for planar geometries;
the effect of axisymmetry for the case of ring vortices;
diffusive viscous effects having their origin at the wall;
secondary vorticity;
finite thickness of the detaching vorticity layer;
the effect of experimental boundedness of rectilinear vortices;
the effect of viscous entrainment as a jet-type flow develops.

Our experiment was designed to single out some of these processes and assess their importance in rendering the flow non-self-similar.

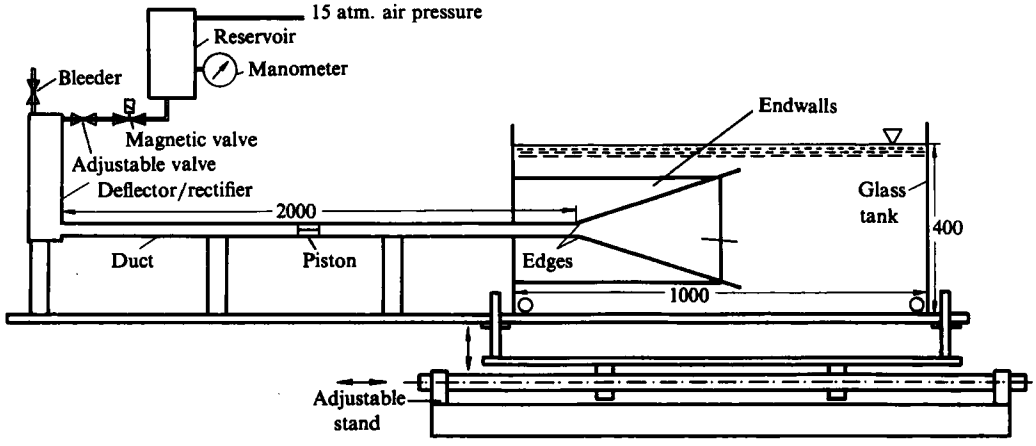

FIGURE 3. Experimental arrangement. Lengths in mm.

3. Experimental arrangement

Figure 3 shows the experimental arrangement. The duct had 10 mm thick walls, roof and floor, and was 2 m long with a height $H = 30$ mm and a width $W = 60$ mm. These dimensions could be reduced by slipping in long pre-cut plates. The 'diffusor' end was submerged in a glass-walled water tank measuring $1 \times 0.4 \times 0.4$ m. The upstream end was connected via a flow rectifier to a valve (to adjust the flow rate), a magnetic valve (≈ 10 ms opening time) and this, in its turn, to a reservoir filled with water under a constant air pressure of up to 15 atm., the whole being free to move in all directions for laser measurements. The temperature of the water remained to within 1° of 19 °C. The adjustable valve allowed $0.5 \leqslant U_p \leqslant 284$ mm/s. The Plexiglas piston was accelerated from rest to its final velocity U_p in less than 40 ms for $U_p = 284$ mm/s. The roof and floor of the last 2 cm of the duct ending at the nozzle plane (see figure 2) were machined from a thickness $d = 10$ to 2 mm (see figure 4). This meant that for the case of $\gamma_r = \gamma_t = \gamma = 0°$, the 'edge' was 2 mm thick. However, microscope glasses 0.1 mm thick (also vital for LDA measurements near the wall) could be used to extend the nozzle, whose 'edges' at the exit then had a thickness $d = 0.1$ mm.

Part of the flow was visualized by letting in an ink/alcohol mixture, either through a 0.4 mm diameter hole drilled from the end of the 2 mm thick wall at the nozzle in the mid-plane, or through a freely movable hypodermic needle of the same diameter. Photographs were then taken with either a Bolex 16H ciné camera operating at between 24 and 64 frames per second, or an electrically-driven Olympus OM2 camera. The x- and y-(laboratory frame) velocity components at various fixed locations were measured with an LDA operating in the dual-scatter mode, using a noise-cancelling difference method described by Bossel, Hiller & Meier (1972).

4.1. *Vortex trajectories*

Figure 4 shows a rolling-up vortex pair photographed from the side (a small secondary vortex due to the relatively thick wall is also visible at the lower edge). Details of the complicated three-dimensional flow associated with vortex generation are discussed in Auerbach (1987). Nonetheless, halving the width W had no effect on the trajectory of the vortex centre in the mid-plane. An average was generally taken over

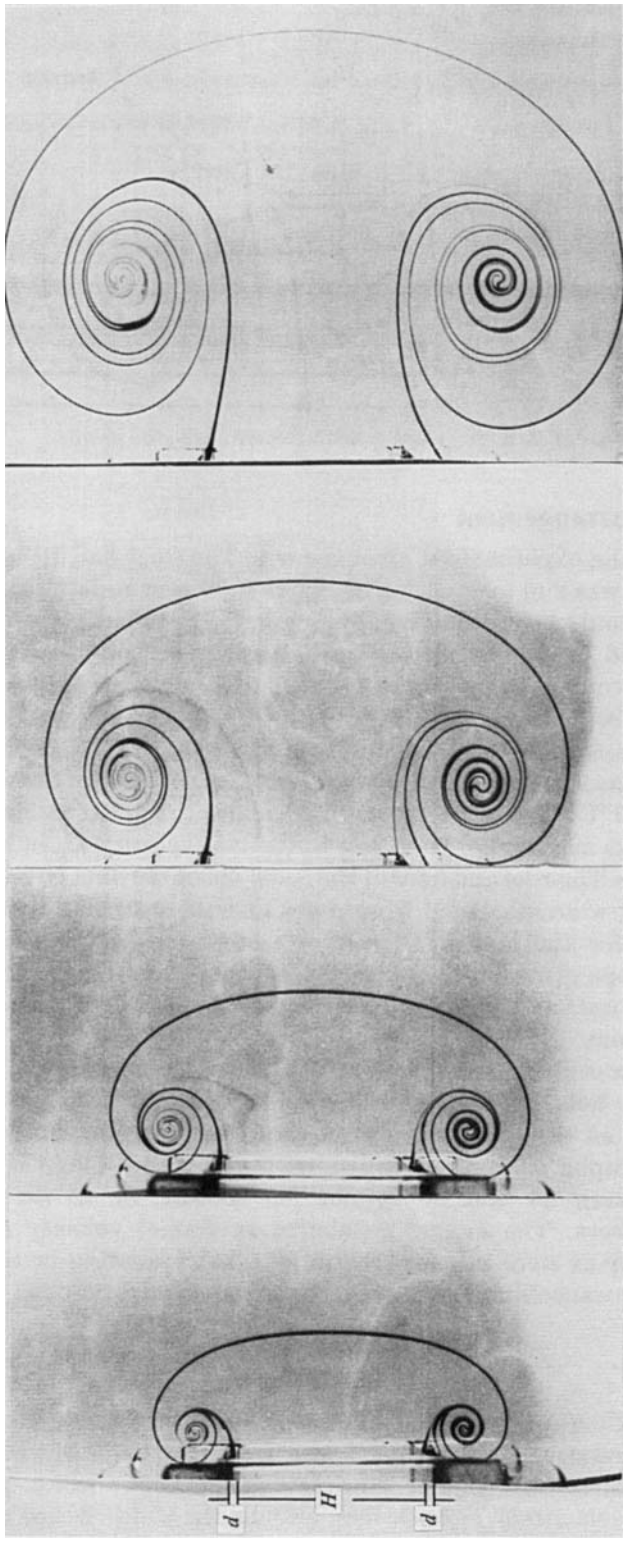

FIGURE 4. Side-on photographs during vortex roll-up dyed in the mid-plane at the edge. $U_p = 40$ mm/s; $d = 2$ mm; $\gamma = 0°$; $W = 60$ mm; $H = 30$ mm; $t = 0.75$, 1, 2 and 4 s. Note the small secondary vortex due to the thick nozzle.

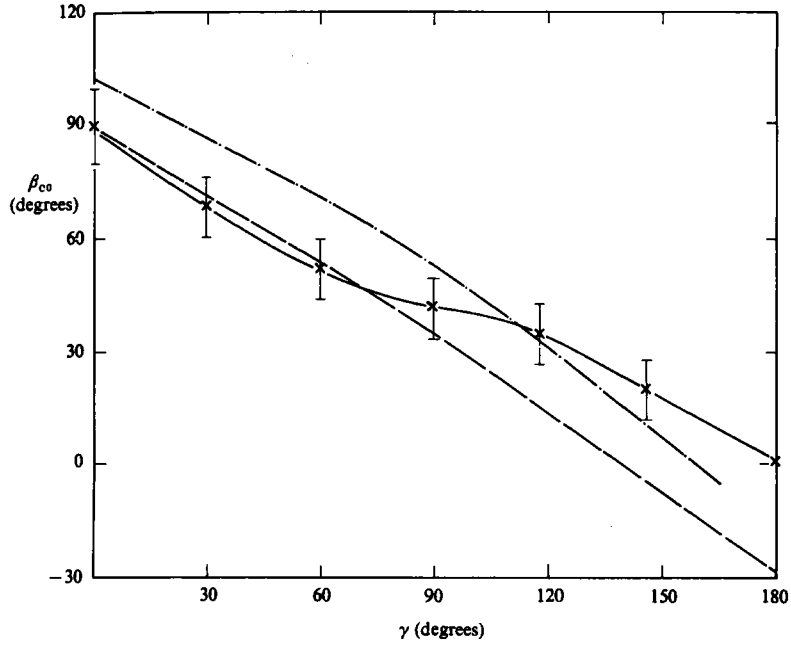

FIGURE 5. The initial angle β_{c0} which the vortex makes to the edge for various edge angles γ, together with theoretical predictions: ——, present experiment $U_p > 18$ mm/s, $d = 0, 1$ mm; – – – –, point vortex; —·—, Pullin (1978).

three runs for the trajectory measurements. For low piston velocities ($U_p \leqslant 5$ mm/s) the positive primary vorticity (see figure 1*b*) detaching from within the upper edge showed no sign of roll-up, the flow detaching effectively steadily, in laminar-jet fashion, from the beginning of the motion. On increasing the piston velocity this vorticity rolled up into a concentrated vortex with a well-defined centre. Figure 5 shows the dependence of the initial angle β_{c0} – that angle β_c shown in figure 1 at that moment when the centre first becomes definable – on the edge angle γ. For the case $\gamma = 0°$ secondary negative vorticity detaching from above the upper edge was simply incorporated into the primary vortex without showing any sign of roll-up in its own sense. However, for $60° \leqslant \gamma \leqslant 150°$ this secondary vorticity rolled up to form its own centre at virtually the same time as the primary vortex was definable. The experimental curve seems to flatten out in this region, having a turning point in the region of $\gamma = 90°$.

For piston velocities $284 \geqslant U_p \geqslant 18$ mm/s the initial angle was independent of the piston velocity. The two dashed lines are theoretical predictions: the lower, almost straight, line is the point-vortex solution (5). The upper line stems from Pullin's (1978) calculations, which include the effect of the rolling-up vortex sheet. As can be seen, the point-vortex solution agrees very well with our experimental results for small edge angles. Pullin's results, on the other hand, agree better for larger edge angles, the point-vortex model predicting a path at 30° to a straight-angled 'edge'. Since Pullin's (1978) theory is without secondary vorticity, it is noteworthy that he obtains best agreement where the secondary vortex is more pronounced.

Let us now consider the components of the trajectory. In general ($284 \geqslant U_p \geqslant 30$ mm/s) the time power laws for the x- and y-coordinates (laboratory and edge-based frames being identical for $\gamma = 0°$) are essentially the same as those

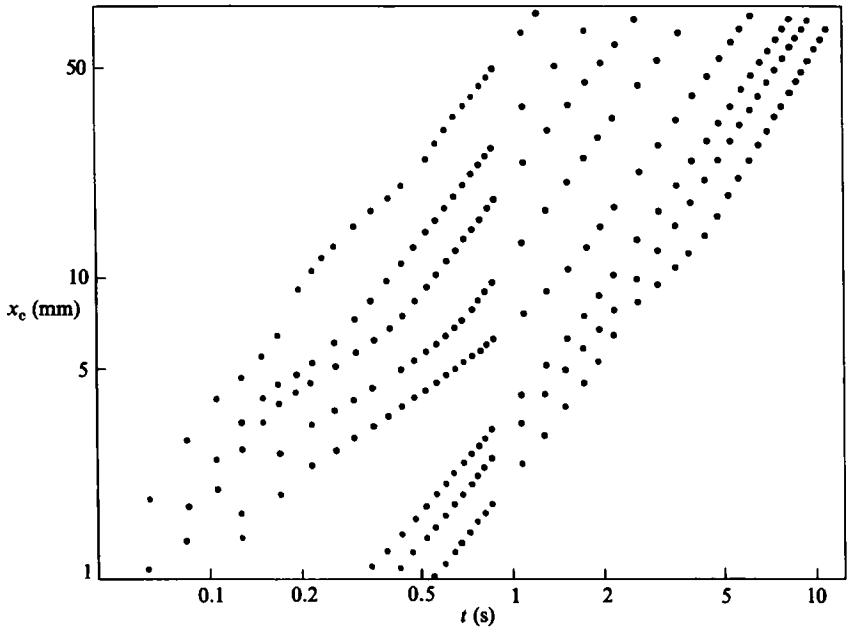

FIGURE 6. Effect of changing the piston velocity on the x-component of the vortex trajectory, $\gamma = 0°$. U_p (from left to right): 284; 192; 120; 80; 46; 30; 24; 18 mm/s.

found by Didden (1979) for ring vortices, namely $x \sim t^{\frac{2}{3}}$ and $y \sim t^{\frac{2}{3}}$. The time power for the y-component is the same as that predicted by (6). Our experimentally found law $y = (U_p^{0.79} t)^{\frac{2}{3}}$ is nonetheless different from $y = (U_p t)^{\frac{2}{3}}$ ((6) with $U_p = V$). No such comparison is possible for the x-component, for its time power is much larger than $\frac{2}{3}$. Figure 6 shows the x-coordinates of the path. For larger piston velocities each curve shows an initially decreasing (from $\frac{2}{3}$) time power, which then however increases to its initial value, the increase beginning at a time $t \approx 1.6H/U_p$. Finally, on extending the lower edge to the end of the duct by adding a plate, we could essentially duplicate Blondeaux & De Bernadinis' (1983) geometry as a special case. For $t < t_e$ the inclusion of this plate did not change the trajectories, indicating that this particular form of distant geometry is not responsible for the non-self-similarity of the flow.

4.2. *Circulation produced at the edge*

In order to ascertain the vorticity, and thus the circulation passing the nozzle plane in the mid-plane (see figure 2), a number of velocity measurements were made in the mid-plane using an LDA, each measurement lasting 2 s. The u-component was measured in the nozzle plane at the following positions within the upper nozzle wall ($y = 30$ mm): $y = 29.80$, 29.52, 29.30, 29.96, 28, 27, 26 and 25 mm. These measurements enabled us to calculate the $(\partial u/\partial y)$-term of the vorticity. The $(\partial v/\partial x)$-term of the vorticity was obtained by measuring the v-component of the velocity 1 mm upstream, as well as 1 mm downstream of the nozzle plane. Such sets of measurements were taken for piston velocities $U_p = 18$, 30 and 46 mm/s for $\gamma = 0°$, and $U_p = 30$ mm/s for $\gamma = 90°$. From the development of the vorticity the circulation could be calculated (cf. Didden 1979).

Figure 7 shows this circulation as a function of time. One sees that, although it is initially substantially smaller than similarity-theory predictions, the virtually

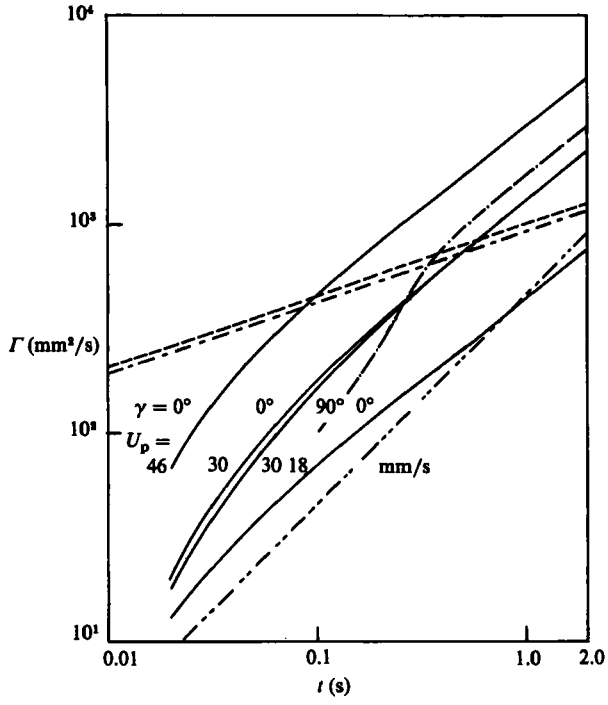

FIGURE 7. Circulation as a function of time for various edge angles γ and piston velocities U_p. ——, Present experiment (see graph for parameters); —·—, Didden (1979), $\gamma = 0°$, $U_p = 46$ mm/s. $\gamma = 0°$, $U_p = 30$ mm/s: – – –, Pullin (1978); – – –, point vortex; ——–, slug-flow model.

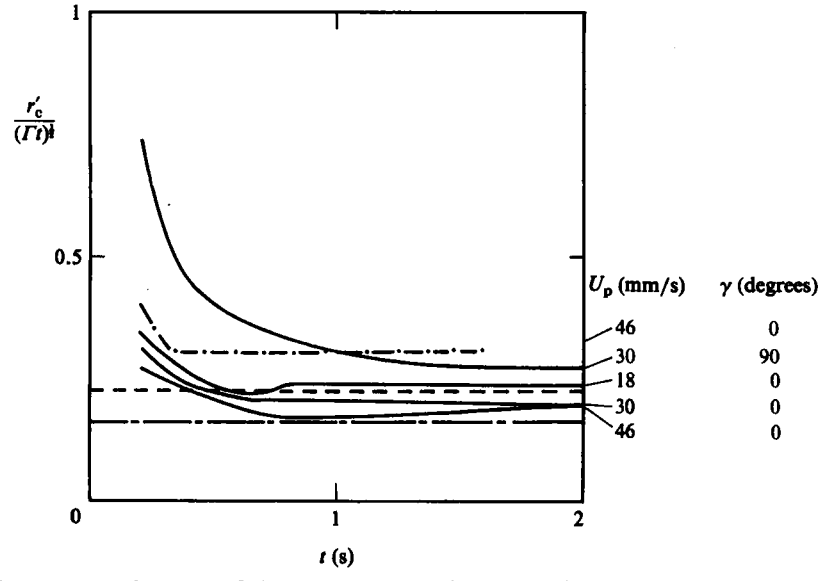

FIGURE 8. Non-dimensional distance of the vortex centre from the edge for various edge angles γ and piston velocities U_p. ——, Present experiment; —·—, Didden (1979); – – –, Pullin (1978); – – –, point vortex.

constant slopes at later times are substantially steeper than those predicted by (7), and far closer to those predicted by the slug-flow model of $\Gamma = 0.5U_p^2 t$. Further, the two curves for $U_p = 30$ mm/s are very close to each other, indicating a virtual independence of the circulation on the edge angle γ at that speed.

We can now plot the non-dimensionalized distance $r_c'/(\Gamma t)^{\frac{1}{2}} = |z_c|/(\Gamma t)^{\frac{1}{2}}$ as shown in figure 8. As can be seen, for large times our curves converge to Pullin's (1978) predictions including the spiral somewhat more closely than they do to predictions due to the point-vortex model. It is surprising that there is any agreement whatsoever between the theories and the experiment, considering the large differences between them for both the circulation and the x-component of the trajectory.

The experimental curves deviate sharply from the theoretical ones for small times, the non-dimensional distance being greater than that predicted by theory; this appears to be related to the discrepancy between theory and experiment in the magnitude of the initial circulation. The deviation is greatest for $\gamma = 90°$, owing to the relatively small effect of changing the edge angle on the circulation production rate in the experiment (see figure 7).

From figure 8 we see that Didden's (1979) non-dimensionalized distance for rings is much larger than ours (both with $U_p = 46$ mm/s) for longer times. Now, his acceleration time was 240 ms, ours 20 ms. The behaviour of the secondary vorticity (rolling/not rolling up) may be influenced by the different histories, although this is not visible in the trajectories. Nonetheless one might expect this influence to become less significant with time. The other possibility lies in the difference in geometries, mentioned in §2. For the case of a ring vortex the effect of the neighbouring vortex element would induce an additional translational velocity from the very beginning of the motion. Now once the vortex has receded from the edge, one might expect the ratio of the translational velocity of the ring to the pair to be $O[\log 8R/c]$. Didden (1977) gives a core radius of 6.4 mm to a ring of radius 32 mm, yielding 3.7 for the above ratio (carried out on a ring with a $U_p = 111$ mm/s). From figure 8 we see that at $t = 1$ s, by which time the y-motion has ceased, and the ratio of the non-dimensionalized distance of the ring to the pair is 1.8, having decreased to 1.6 at $t = 2$ s. Further, from figure 7, after 0.5 s the pair-to-ring circulation ratio is $\frac{6}{3}$, yielding a pair-to-ring distance ratio of 2.1. Since the time powers for rings and pairs are the same, both for the circulation production as well as for the x-trajectory, this ratio is also the ring-to-pair translational-velocity ratio. The effect is there, but the value is somewhat low. As discussed earlier, Pullin's (1978) theory takes the difference in the geometry into account by the constant q in the lengthscale in the form of (2) as initially discussed. His formulation for the vortex generation leaves q in the lengthscale, extracting p – the vortex-model-dependent parameter – from the lengthscale, and dividing it into two model-dependent factors C and Ω. His formulation for the relation between Γ and s then leads to the non-dimensional radius above being vortex-model dependent but independent of the geometry – an unjustifiable result because of the above experimentally found mutual influence for rings.

5. Why is vortex roll-up non-self-similar?

Let us first collect our main results.

Vortex pairs and rings have similar initial non-self-similar trajectories.

A wall introduced far from the salient edge does not affect the initial trajectory.

The existence of the endwalls does not affect the trajectory.

Changing the edge angle γ has relatively little effect on the circulation (figure 7).

The predicted initial circulation (figure 7) is too large.

The predicted slope for the circulation (figure 7) is too small.

The self-induced velocity due to the curvature of ring vortices is significant.

At the outset we mentioned seven possible processes that may be important for the non-self-similar behaviour of the starting vortex. Some of these may now be ruled out with a measure of certainty. The idea that a distant geometry, such as those mentioned by Blondeaux & De Bernadinis (1983), affects the initial flow, does not seem correct. Further Didden's (1979, 1982) suggestion, that the axisymmetry of the geometry affects the self-similarity, seems also not to be borne out by experiment. As to effects of diffusive viscous origin, although they must affect the initial flow, the times in which these are active are so small that it seems unlikely that they could affect the flow significantly. The endwalls seem to have no effect on the trajectory of the vortex centre in the mid-plane.

The existence of secondary vorticity will have two immediate effects on the flow. It will tend to thicken the ejected shear layer and will tend to roll-up in its own sense. The effect of the thickness might be expected not to be large once the vortex structure is large in comparison. It will, however, reduce the effective circulation of the vortex (in figure 7 circulation generated above the nozzle was not included). As to the time-power law of the vortex centres, there is a similarity between the initial motion and that when the vortex begins being affected by the entraining motion of the developing jet. The centres of faster moving vortices move along an initially curved trajectory, straightening out for a while before again following a curved path. Since the power to which the y-component of the trajectory must be raised remains $\frac{2}{3}$, this change is reflected entirely by the changing time power for the x-component, being initially $\frac{3}{2}$, then briefly reducing for higher piston velocities, again increasing to take on its initial value of $\frac{3}{2}$. We saw from figure 6 that this increase takes place at approximately $t = t_e = 1.6H/U_p$, and seems to be associated with the moving vortex becoming aware of its partner in a field that changes its character from that of an edge flow to that of the entraining jet discussed earlier. Yet at the beginning of the motion, the detached (and, for certain geometries, rolling-up) secondary circulation is of an intensity comparable with that of the primary vortex (25% for ring vortices, Didden 1979), and we have a true (albeit tiny) vortex pair at the edge, rather than a single vortex. One possible interpretation for the initial $\frac{3}{2}$-value is that the negative leeward vorticity acts in the same way for the beginning of the trajectory as does its partner for $t > t_e$. At this stage however, one cannot conclude which of the effects, secondary vorticity (in particular when rolling up) or viscous entrainment, is more important. One might then interpret the reduction in the power (towards $\frac{2}{3}$?) as indicating a tendency for the flow to follow (4), the similarity-theory prediction.

Finally, what is the effect of rolled-up secondary vorticity on the circulation? Insofar as it is reasonable to replace a detached boundary layer with a boundary, the most obvious effect of the former is that it will change the effective geometry at the edge, tending to make the sharp edge blunter. This means that rolled-up secondary vorticity will tend to increase the value of γ, as well as reduce the effect of changing γ on the circulation. From (7), increasing γ from 0° to 180° increases the power to which the time is raised from $\frac{1}{3}$ to 1. On the other hand one can show that the coefficient of t decreases for all times $t < 3.7$ s. Both these tendencies are present in our experiments.

On the basis of the above discussion it seems that the simple potential approach used does not adequately describe the motion of the starting vortex. Either the basic

flow or the vortex model are at fault. The basic flow onto which the vortex is superposed may well not be a pure edge flow, but one that already has the character of an entraining jet flow. On the other hand, the vortex model fails to incorporate secondary vorticity which, particularly when rolled up, might be expected to be dynamically important.

I should like to thank Ernst-August Müller for his help in this research during all stages in its development; the reviewers, for their painstaking criticisms; Horst Vogel, for a number of clarifying discussions and the Deutsche Forschungsgemeinschaft, for its financial support.

REFERENCES

AUERBACH, D. E. 1987 Some three-dimensional effects during vortex generation at a straight edge. *Exp. Fluids* (in press).

BLONDEAUX, P. & DE BERNADINIS, B. 1983 On the formation of vortex pairs near orifices. *J. Fluid Mech.* **135**, 111–122.

BOSSEL, H. H., HILLER, W. J. & MEIER, G. E. A. 1972 Noise-cancelling signal difference method for optical velocity measurements. *J. Phys.* E: *Sci. Instrum.* **5**, 893–1096.

BROWN, C. E. & MICHAEL, W. H. 1955 On slender delta wings with leading edge separation. *NACA Tech. Note* 3430.

CHOW, C.-Y. & HUANG, M.-K. 1982 The initial lift and drag of an impulsively started aerofoil of finite thickness. *J. Fluid Mech.* **118**, 393–409.

DIDDEN, N. 1977 Untersuchung laminarer, instabiler Ringwirbel mittels Laser-Doppler-Anemometrie. *MPI/AVA Bericht* 64.

DIDDEN, N. 1979 On the formation of vortex rings: rolling-up and production of circulation. *Z. Angew. Math. Phys.* **30**, 101–115.

DIDDEN, N. 1982 On vortex formation and interaction with solid boundaries. In *Vortex Motion* (ed. H. G. Hornung & E.-A. Müller), pp. 1–17. Braunschweig: Vieweg.

GRAHAM, J. M. R. 1977 Vortex shedding from sharp edges. *IC Aero-Rep.* 77-01. Imperial College of Science and Technology.

GRAHAM, J. M. R. 1983 The lift on an aerofoil in starting flow. *J. Fluid Mech.* **133**, 413–425.

KADEN, H. 1931 Aufwicklung einer unstabilen Unsetigkeitsfläche. *Ing.-Arch.* **2**, 140–168.

KRAEMER, K. 1971 Die Potentialströmung in der Umbgebung von Freistrahlen. *Z. Flugwiss.* **19**, 94–104.

PULLIN, D. I. 1978 The large-scale structure of unsteady self-similar rolled-up vortex sheets. *J. Fluid Mech.* **88**, 401–430.

PULLIN, D. I. 1979 Vortex generation at tube and orifice openings. *Phys. Fluids* **22**, 401–403.

PULLIN, D. I. & PERRY, A. E. 1980 Some flow visualization experiments on the starting vortex. *J. Fluid Mech.* **97**, 239–255.

TAYLOR, G. I. 1958 Flow induced by jets. *J. Aero/Space Sci.* **25**, 464–465.

WALKER, J. D. A. 1978 The boundary layer due to a rectilinear vortex. *Proc. R. Soc. Lond.* A **359**, 167–188.

WEDEMEYER, E. 1961 Ausbildung eines Wirbelpaares an den Kanten einer Platte. *Ing.-Arch.* **30**, 187–200.